0026-895X/07/7106-1695–1702$20.00
MOLECULAR PHARMACOLOGY
Copyright © 2007 The American Society for Pharmacology and Experimental Therapeutics
Mol Pharmacol 71:1695–1702, 2007

Vol. 71, No. 6
33845/3213774
Printed in U.S.A.

The Thiazolidinedione Pioglitazone Alters Mitochondrial Function in Human Neuron-Like Cells

Sangeeta Ghosh, Nishant Patel, Douglas Rahn, Jenna McAllister, Sina Sadeghi, Geoffrey Horwitz, Diana Berry, Kai Xuan Wang, and Russell H. Swerdlow

Department of Neurology, University of Virginia School of Medicine, Charlottesville, Virginia

Received December 29, 2006; accepted March 26, 2007

ABSTRACT

Thiazolidinediones alter cell energy metabolism. They are used to treat or are being considered for the treatment of disorders that feature mitochondrial impairment. Their mitochondrial effects, however, have not been comprehensively studied under long-term exposure conditions. We used the human neuron-like NT2 cell line to directly assess the long-term effects of a thiazolidinedione drug, pioglitazone, on mitochondria. At micromolar concentrations, pioglitazone increased mitochondrial DNA (mtDNA) content, levels of mtDNA and nuclear-encoded electron transport chain subunit proteins, increased oxygen consumption, and elevated complex I and complex IV V_{max} activities. Pioglitazone treatment was also associated with increased cytoplasmic but reduced mitochondrial peroxide levels. Our data suggest that pioglitazone induces mitochondrial biogenesis and show that pioglitazone reduces mitochondrial oxidative stress in a neuron-like cell line. For these reasons pioglitazone may prove useful in the treatment of mitochondriopathies.

The thiazolidinedione compound pioglitazone reduces insulin resistance in persons with type II diabetes (Yki-Järvinen, 2004). It agonizes a transcription-activating protein, peroxisome proliferator activator receptor (PPARG). Pioglitazone thus mimics the affects of PPARG's physiologic coactivator, peroxisome proliferator-activated receptor [coactivator 1α (PGC-1α)]. Recent data indicate PGC-1α also coactivates another transcription activating protein, nuclear respiratory factor 1 (NRF-1) (Wu et al., 1999; Scarpulla, 2002). NRF-1 initiates expression of nuclear-encoded components of the mitochondrial electron transport chain (ETC) and facilitates mitochondrial proliferation. For this reason, it seems reasonable to consider the effects of pioglitazone on mitochondria.

Data suggest that thiazolidinediones directly affect mitochondrial function (Dello Russo et al., 2003). For example, previous work suggests that thiazolidinediones may affect coupling-uncoupling dynamics (Digby et al., 1998; Kelly et al., 1998; Shimokawa et al., 1998). These drugs seem to decrease oxidative phosphorylation coupling, which could in turn increase glucose utilization and influence free radical production/oxidative stress. The effects of thiazolidinediones on oxidative stress are difficult to predict. Uncoupling can be associated with reduced free radical production (Fiskum et al., 2004). On the other hand, the ability of short-term thiazolidinedione exposure to increase oxidative stress has been reported (Shishido et al., 2003). To complicate matters, thiazolidinediones may affect mitochondria through more than one mechanism (Feinstein et al., 2005).

Thiazolidinediones are currently under consideration for the treatment of Alzheimer's disease (AD) (Landreth, 2006). The most proposed rationale is that thiazolidinedione anti-inflammatory properties may prove useful for mitigating β amyloid-induced microglial activation, a process potentially contributing to neurodegeneration. Mitochondrial dysfunction is also a well documented feature of AD (Parker et al., 1990; Swerdlow and Kish, 2002; Roses et al., 2007). Whether a primary or secondary phenomenon in AD, mitochondrial dysfunction in AD permits its designation as a mitochondriopathy (Swerdlow, 2007). Because of this, we chose the NT2

This research was funded by grants from Takeda Pharmaceuticals and the National Institute on Aging (AG022407).
Article, publication date, and citation information can be found at http://molpharm.aspetjournals.org.
doi:10.1124/mol.106.033845.

ABBREVIATIONS: PPARG, peroxisome proliferator activator receptor; PGC-1α, peroxisome proliferator-activated receptor (coactivator 1α); NRF-1, nuclear respiratory factor 1; ETC, electron transport chain; AD, Alzheimer's disease; DMSO, dimethyl sulfoxide; PBS, phosphate-buffered saline; PMSF, phenylmethylsulfonyl fluoride; HBSS, Hanks' buffered salt solution; mtDNA, mitochondrial DNA; NRF, normalized relative fluorescence; NT2, Ntera/D1; DTNB, 5,5′-dithio-bis (2-nitrobenzoic acid); DCF, 2′,7′-dichlorodihydrofluorescein diacetate; HRP, horseradish peroxidase; H_2O_2, hydrogen peroxide; GPx, glutathione peroxidase; DC, detergent compatible; DTT, dithiothreitol; TBS, Tris-buffered saline; PCR, polymerase chain reaction; ETC, electron transport chain.

neuron-like cell line for studying how long-term pioglitazone exposure affects mitochondrial function.

Materials and Methods

Cell Culture. Human teratocarcinoma Ntera/D1 (NT2) neuronal precursor cells were maintained and expanded in 75-cm^2 flasks at 37°C and 5% CO_2. Our NT2 cells were originally obtained from Stratagene (La Jolla, CA). The maintenance medium consisted of Opti-MEM (Invitrogen, Carlsbad, CA) supplemented with 10% heat-inactivated, nondialyzed fetal bovine serum and 1% penicillin-streptomycin.

Pioglitazone-containing media were prepared through addition of a sterile pioglitazone stock solution. The stock solution consisted of pioglitazone powder (Takeda Pharmaceuticals, Osaka, Japan) dissolved in dimethyl sulfoxide (DMSO). This stock was prepared as a 20 mM solution (15.7 mg in 2 ml of DMSO). Pioglitazone-containing media contained final concentrations of 10, 20, or 40 μM pioglitazone; for some parameters, 5 μM pioglitazone was also evaluated. To control for the DMSO vehicle, 1 ml of DMSO was added to 500 ml of the 0 μM medium.

Cells were maintained in their designated medium for at least 2 weeks before any assays. Cells were harvested when flasks reached 90% confluence. We also routinely changed the culture medium 1 day before harvesting. Adherent cells were detached by washing the flask surface with phosphate-buffered saline (PBS) followed by trypsinization. Detached cells were placed in 15-ml conical tubes (for whole-cell applications) or 50- ml conical tubes (for applications requiring isolated mitochondria). The larger volume tubes were used for mitochondrial isolation because for this, we routinely combined the contents of at least two flasks. After trypsin was removed by a 5-min centrifugation at 200*g* (4°C), the cells were washed twice in PBS and pelleted via centrifugation (5 min, 200*g*, 4°C).

Mitochondrial Enrichment. Mitochondrial isolation was performed at 4°C. Washed cell pellets were prepared as described above. These pellets were suspended in isolation buffer (10 mM HEPES, pH 7.3, 1 mM $MgCl_2$, and 0.25 M sucrose) containing fresh protease inhibitors (Protease Inhibitor Cocktail Set I; Calbiochem, San Diego, CA) and 200 μM phenylmethylsulfonyl fluoride (PMSF). The contents of at least two confluent T75 flasks were combined before cell rupture, and we used 2 ml of isolation buffer for each harvested flask. Suspended cells were disrupted in a prechilled, 45-ml nitrogen cavitation chamber (Parr Instrument Company, Moline, IL) at 600 psi for 10 min. Cells were constantly stirred during the pressurization period. The cavitation chamber contained a discharge valve. At the end of the pressurization period, the contents were eluted through the discharge valve and collected in a 15-ml conical polypropylene tube. An additional 2 ml of isolation buffer (not supplemented with protease inhibitors or PMSF) was then used to rinse the inside of the cavitation chamber and poured out the open discharge valve into the tube containing the previously eluted pressurized cells. Undisrupted cells and nuclei were pelleted for removal by centrifugation at 1000*g* for 10 min. An aliquot of the postnuclear supernatant, which contained cytoplasmic contents and ruptured membranes, was set aside for glutathione peroxidase (GPx) assays. The rest of the supernatant was centrifuged at 9000*g* for 10 min. The resulting crude mitochondrial pellet was suspended in 400 μl of isolation buffer. Protein content of either the 1000*g* supernatant or mitochondrial fraction was determined using the DC protein assay (Bio-Rad Laboratories, Hercules, CA).

Cytochrome Oxidase, Citrate Synthase, and Complex I V_{max} Assays. Cytochrome oxidase and citrate synthase activities were determined on the whole-cell pellets described above. These pellets were suspended in Ca^{+2}/Mg^{+2}-free Hanks' buffered salt solution (HBSS) (Gibco BRL) at a concentration of 30×10^6 cells/ml. Protein content of the whole-cell suspensions was determined using the DC protein assay. For the cytochrome oxidase assay, a cuvet containing potassium phosphate buffer (20 mM, pH 7.0), dodecyl maltoside (20 μl from a 10 mg/ml stock solution), and 25 μg of cell protein was warmed to 30°C for two min. The reaction was initiated by addition of 25 μM reduced cytochrome *c*, which brought the total cuvet volume to 1 ml. The oxidation of the reduced cytochrome *c* was followed for 2 min at 550 nm on a DU series spectrophotometer (Beckman Coulter, Fullerton, CA). To facilitate calculation of enzyme activity, the maximally oxidized cytochrome *c* absorbance was determined by adding several grains of potassium ferricyanide to the cuvet. The apparent first-order rate constant was calculated and normalized to the amount of protein added to the cuvet (seconds^{-1} per milligram of protein). At least 12 independent assays were performed for each condition.

For citrate synthase activity determinations, a cuvet containing 100 mM Tris, pH 8.0, 100 μM DTNB [5,5′-dithio-bis (2-nitrobenzoic acid)], 0.04% (v/v) Triton X-100 (added as 4 μl of a 10% Triton solution), and 40 μg of cell suspension was warmed over 2 min to 30°C. The reaction was initiated by the addition of first 100 μM oxaloacetate and then 50 μM acetyl CoA. The total cuvet volume was 1 ml. Citrate synthase catalyzes the release of a thiol from acetyl CoA, which reacts with DTNB to form 5-mercapto-2-nitrobenzoic acid. The extinction coefficient of DTNB reduction is 0.0136 $\mu M^{-1}cm^{-1}$. The resulting absorbance change was followed in a spectrophotometer for 2 min at 412 nm. This absorbance change was divided by the extinction coefficient, and this value was further divided by the amount of protein in the cuvet. Citrate synthase activities were thus recorded as activity per milligram of protein (nanomoles per minute per milligram of protein). Ten independent assays were performed for each condition.

Complex I activities were determined from crude mitochondrial fractions (prepared as described above). Immediately after suspension of the mitochondrial pellet in 400 μl of isolation buffer, 100 μl was taken for protein determination using the DC protein assay. The remaining 300 μl were transferred to 1-ml polystyrene centrifuge tubes (Fisherbrand; Fisher Scientific, Pittsburgh, PA), and these tubes were tightly capped. The mitochondria in the polystyrene tubes were then subjected to one freeze-thaw cycle, which was accomplished by cooling the suspension to −80°C for 1 to 2 h. After thawing, the capped tubes containing the mitochondrial suspensions were sonicated in the cup horn of a W-225 sonicator (Heat Systems-Ultrasonics, Farmingdale, NY). During the sonication procedure, the cup horn was also filled with an ice-water slurry, and the polystyrene tubes were maintained in a horizontal orientation 1 cm above the base of the cup horn. It is important to note when disrupting mitochondria through closed tubes that optimal sonication parameters depend on tube material and sonicator type. For the sonicator and polystyrene tubes we used, we found a 6-min sonication at 50% duty cycle and output control of 7 provided optimal mitochondrial disruption.

A cuvet containing complex I assay buffer (25 mM KPO_4, pH 7.4, 0.25 mM potassium EDTA, and 1.5 mM KCN) and 10 μl of a 10 mM β-NADH stock solution was warmed over 2 min to 30°C. The NADH stock solution was prepared using complex I buffer. After this 2-min warming period, 100 μg of sonicated mitochondrial protein was added to the cuvet, which was then warmed for an additional minute at 30°C. The reaction was initiated by addition of coenzyme Q1 (Sigma-Aldrich, St. Louis, MO) to a final cuvet concentration of 60 μM. The coenzyme Q1 was added from a stock solution in which coenzyme Q1 was dissolved in ethanol at a concentration of approximately 25 mM. The final cuvet volume was 1 ml.

Our complex I assay used a spectrophotometer to follow the decrease in NADH absorbance that occurs at 340 nm as NADH is oxidized by complex I to NAD+. We followed this absorbance change over 2 min at 30°C. To account for NADH oxidation by other NADH oxidases, after 2 min we added 20 μM rotenone (10 μl from a 2 mM stock solution in which the rotenone was dissolved in methanol) to the cuvet and tracked the change in 340 nm absorption for another 2 min. The postrotenone rate was subtracted from the prerotenone rate to yield the rotenone-sensitive rate. In general, the rotenone-sensitive rate accounted for 80 to 90% of the total rate. The rotenone-sensitive rate was divided by 0.00681 $\mu M^{-1}cm^{-1}$, the combined

NADH-Q1 extinction coefficient at 340 nM. This value was then divided by the amount of protein in the cuvet to provide the rotenone-sensitive rate as nanomoles per minute per milligram of protein. At least 15 independent assays were performed for each condition.

Cell Oxygen Consumption. Whole cells were harvested and washed as described above. The whole cell pellets were then suspended in PBS at a concentration of 30×10^6 cells/ml. 200 μl of each cell suspension was placed in individual wells of a BD Oxygen Biosensor System plate (BD Biosciences, San Jose, CA). Each suspension was run in triplicate. BD Oxygen Biosensor System plates contain a dye that fluoresces with exposure to dissolved oxygen. Plates were scanned using a Victor2 plate reader (PerkinElmer Life and Analytical Sciences, Boston, MA) with an excitation wavelength of 485 nm and an emission wavelength of 630 nm. Readings were taken at 30 min intervals for a total of 2 h. The plate was kept at 37°C and 5% CO_2 between readings. Data were normalized according to the manufacturer's normalization protocol (technical bulletin 448; BD Biosciences), which converted the data to normalized relative fluorescence (NRF) units. We then divided the calculated NRF units by the amount of protein added to each well. Our data are thus presented as NRF units per milligram of protein. The three replicates for a given whole-cell suspension were averaged to provide a single data point. The total NRF unit means for the independently analyzed cell suspensions of a particular condition were determined at 1 h. Over the 2-h reading period, there was a linear fluorescence increase, and the mean NRF unit slopes for the independently analyzed cell suspensions of a particular condition were calculated. At least 10 independent whole-cell suspensions were assayed for each condition.

Oxidative Stress Determinations. Cytoplasmic peroxide levels were estimated using 2′,7′-dichlorodihydrofluorescein diacetate (DCF) (Molecular Probes, Inc., Eugene, OR). For this assay, cells were harvested and washed as described above. The washed whole-cell pellets were suspended in a freshly prepared dye loading buffer consisting of HBSS (containing calcium and magnesium but not phenol red), 2 μM DCF, and 0.1 μg/ml Hoechst 33342 (Molecular Probes, Inc.). These suspensions were maintained in the dark for 30 min at 37°C and 5% CO_2. At the end of this dye loading period, the cells were pelleted by centrifugation. The cell pellet was suspended in HBSS (containing calcium and magnesium but not phenol red) containing no dyes and the cells were repelleted. The washed cells were then suspended in assay buffer (PBS supplemented with 20 mM glucose) at a concentration of 5×10^6 cells/ml. Two hundred microliters from each cell suspension (1×10^6 cells) were added to individual wells of a clear 96-well plate (Fisherbrand; Fisher Scientific). Each suspension was assayed in triplicate. The plates were analyzed using a Victor2 fluorescence plate reader at two different settings. The first setting, with excitation at 485 nm and emission at 530 nm, measured DCF fluorescence. The second setting, with excitation at 355 nm and excitation at 460 nm, measured Hoechst fluorescence. Hoechst stains cell nuclei and its fluorescence provides a linear correlate of the number of cells in a well. The Hoechst readings were done to ensure differences in the number of cells added to each well did not account for differences in DCF fluorescence. After dividing the DCF fluorescence of each well by its Hoechst fluorescence, we averaged the three wells for each sample to obtain a final value. Plates were read at 10-min intervals over 1 h. Between readings, plates were kept in the dark at 37°C and 5% CO_2. Fluorescence increase slopes were calculated that reflect increasing DCF fluorescence, because Hoechst fluorescence did not change between readings. Results for each pioglitazone condition are expressed as its fluorescence increase slope relative to that of pioglitazone-untreated cells. Eleven independent measurements were made for each condition.

Mitochondrial peroxide production was assessed using the Amplex red (10-acetyl-3,7-dihydroxyphenoxazine) reagent. For this assay, we used isolated mitochondria, which were prepared as described above. After suspending crude mitochondria pellets in 400 μl of isolation buffer, we used the Bio-Rad Laboratories DC protein assay to determine the protein concentration of each suspension. Based on these protein determinations, we added specific amounts of additional isolation buffer (without protease inhibitors or PMSF) to the suspensions of each group so that the final protein concentrations for all the suspensions in a group were equivalent. Stock solutions for glutamate (500 mM in water), malate (500 mM in water), ADP (500 mM in water), Amplex red (10 mM in DMSO), and horseradish peroxidase (HRP; 10 U/ml in kit reaction buffer) were made. All stock solutions except the HRP solution were 100× their working concentrations; the HRP stock solution was 50× its working concentration. To prepare 1 milliliter of working solution, 10 μl each of the glutamate, malate, ADP, and Amplex red stocks were added to 20 μl of the HRP stock and 940 μl of isolation buffer (without protease inhibitors or PMSF). The working solution therefore contained 5 mM glutamate, 5 mM malate, 5 mM ADP, 100 μM Amplex red, and 0.2 U/ml HRP. To initiate the assay, 50 μl of working solution were added to 50 μl of mitochondrial suspension in clear 96-well microtiter plates. The plates were analyzed with a Wallac Victor2 fluorescence plate reader using excitation at 560 nm and emission at 590 nm. Readings were taken at 1-min intervals. Thirty readings were taken. Each suspension was measured in triplicate and mean values for each suspension were determined for each time point. Amplex red reacts with H_2O_2 to produce highly fluorescent resorufin. The slope of the resorufin fluorescence increase was calculated for each sample. The slopes for the suspensions containing mitochondria from pioglitazone-treated cells were compared with the slopes of suspensions containing mitochondria from pioglitazone-untreated cells. At least 10 independent assays were performed for each pioglitazone concentration.

The glutathione peroxidase (GPx) reaction follows the oxidation of NADPH to NADP+, which manifests as an absorbance decrease at 340 nm. We performed our measurements with a DU series spectrophotometer (Beckman Coulter). First, NT2 cell postnuclear fractions were generated as described above with minor modification. Instead of suspending whole cells in 2 ml per flask before nitrogen cavitation, whole cells were suspended in 1 ml of isolation buffer per flask, and after nitrogen cavitation the chamber was washed with only 1 ml of isolation buffer. This modification was done to concentrate the contents of the postnuclear supernatant generated by the 1000*g* spin. We used postnuclear fractions because GPx is found in both cytoplasm and mitochondria. The protein concentration for each sample was measured using the Bio-Rad Laboratories DC protein assay. Postnuclear fractions were then subjected to one freeze-thaw cycle (frozen at −80°C for at least 2 h). The actual GPx assay was performed using the Total Glutathione Peroxidase Assay Kit (ZeptoMetrix, Buffalo, NY). This kit provides buffers, NADPH, glutathione, glutathione reductase, and cumene hydroperoxide. Assays were performed according to the manufacturer's instructions, with modifications as specified. Instead of adding 30 μl of sample, we adjusted our sample volumes so that 100 μg of postnuclear, freeze-thawed protein was added to the assay cuvet. This tended to require a 50- to 60-μl volume addition. To compensate for this minor increase in sample volume, we reduced the amount of working solution A so that the final assay volume in the cuvet was maintained at 960 μl. In addition, a control was run for each sample in which a corresponding volume of deionized water was substituted for the actual sample. This provided a background rate that was subtracted from the rate obtained with the sample. The final corrected rate for each sample was divided by the NADPH extinction coefficient (0.00622 $\mu M^{-1} cm^{-1}$), and this result was further divided by the amount of protein in the cuvet (0.1 mg). GPx activities from the postnuclear fractions of pioglitazone-treated cells were compared with those of postnuclear fractions from pioglitazone-untreated cells. Data are reported as relative activities. Twelve independent measurements were performed for each condition.

Protein Electrophoresis and Western Blotting. Immunochemical determinations of cytochrome oxidase subunit 1 (CO1) pro-

tein levels were performed using isolated mitochondrial protein. Immunochemical determinations of cytochrome oxidase subunit 4 (CO4) protein levels were performed using whole-cell protein. Mitochondria and whole cell fractions were prepared as described above and suspended in 200 μl of PBS and 200 μl of a 2× Laemmli buffer. The 2× Laemmli buffer was prepared as follows: 10 ml of 1 M Tris-HCl, pH 6.8, 20 ml of 20% SDS, 20 ml of glycerol, and 40 ml of deionized H_2O. Samples were heated at 100°C for 5 min, and protein concentrations were determined using the Bio-Rad Laboratories DC assay. DTT and bromphenol blue were then added to the remaining sample (from a 1 M DTT, 0.1% bromphenol blue stock prepared in 1× Laemmli buffer) in a ratio of nine parts sample to one part DTT/bromphenol blue stock. The sample tube was then heated again at 100°C for 5 min. For CO1 determinations, 20 μg of mitochondrial protein were loaded onto 4 to 20% Tris-HCl polyacrylamide gels (Bio-Rad Laboratories). For CO4 determinations, 10 μg of whole cell protein were loaded onto 4 to 20% Tris-HCl polyacrylamide gels. Gels were electrophoresed for 45 min at 200 V. Proteins were transferred to polyvinylidene difluoride membranes (Bio-Rad Laboratories) using 200 mA for 2 h. The membranes were blocked in Tris-buffered saline [TBS (50 mM Tris base and 150 mM NaCl, pH 7.5)] containing 0.05% Tween 20 and 5% milk for 1 h at room temperature. Membranes were incubated overnight at 4°C with monoclonal antibodies to CO1 or CO4 (Molecular Probes). After stripping, the CO4 blots were later restained with a monoclonal antibody to α-tubulin (Calbiochem). After overnight staining with primary antibodies, membranes were washed four times with TBS containing 0.05% Tween 20 and incubated for 1 h at room temperature with an HRP-conjugated goat anti-mouse antibody (Jackson ImmunoResearch, West Grove, PA). Unbound secondary antibody was removed by four 10-min washes with TBS containing 0.05% Tween 20. The HRP-conjugated secondary antibody was activated with a solution containing an HRP substrate (West Dura Substrate; Pierce, Rockford, IL) and visualized with a Kodak 440 CF Image Station (Eastman Kodak, Rochester, NY). Band densities were determined using Kodak 440CF Image Station software. At least five independent samples were analyzed for each pioglitazone treatment condition, and the mean densities for each condition calculated. Mean densities for the different pioglitazone-treated cell groups were compared with that of the pioglitazone-untreated cell group.

Real-Time PCR. We used real-time PCR to compare relative amounts of mtDNA and nuclear DNA copy numbers within pioglitazone-treated and untreated cells. Amplicons to two different mtDNA regions and one nuclear DNA region were generated for this analysis. The mtDNA amplicons were generated from the CO1 and D-loop segments. The nuclear amplicon was generated through amplification of a β-actin segment. The mtDNA primers were designed to minimize amplification of mtDNA pseudogenes embedded in nuclear DNA (http://www.ncbi.nlm.nih.gov/BLAST), and were obtained from Operon (Operon Biotechnologies, Inc., Huntsville, AL). The CO1 primers were as follows: 5′-ATACTACTAACAGACCGCAACCTC-3′ (forward primer), and 5′-GAGATTATTCCGAAGCCTGGT-3′ (reverse primer). These primers generated a 143-base pair product. The D-loop primers were as follows: 5′-GGAGCACCCTATGTCGCAGTATC-3′ (forward primer) and 5′-TGTCTGTGTGGAAAGTGGCTGTG-3′ (reverse primer). These primers generated a 106-base pair product. The β-actin primers were as follows: 5′-GAAGGATTCCTATGTGGGCGA-3′ (forward primer), and 5′-CAGGGTGAGGATGCCTCTCTT-3′. These primers generated a 103-base pair product.

External standards were prepared as described previously (von Wurmb-Schwark et al., 2002; May-Panloup et al., 2005) with minor modifications. PCR reactions were performed using iProof High Fidelity DNA Polymerase (Bio-Rad Laboratories) and 100 ng of genomic DNA. Thirty cycles of denaturation (30 s at 94°C), primer annealing (30 s at 58°C), and extension (1 min at 72°C) were performed. Amplicons were purified using QIAquick tubes (QIAGEN, Valencia, CA) and quantified with a DU series spectrophotometer (Beckman Coulter). From each of these amplicons, five serial 10-fold dilutions were prepared and stored at −20°C as single-use aliquots.

An iCycler iQ real-time PCR Detection System thermocycler (Bio-Rad Laboratories) was used to perform real-time PCR amplification using iQ SYBR Green Supermix (Bio-Rad Laboratories). One hundred nanograms of genomic DNA was used for each reaction. Mitochondrial to nuclear DNA ratios were calculated by dividing the mtDNA quantity for each sample by its corresponding β-actin quantity. The mtDNA:nuclear DNA ratios from pioglitazone-treated cells were compared with that of untreated cells.

Statistical Analysis. Data are expressed as mean values ± S.E.M. for all independent assays of a particular condition. Two-tailed Student's t tests were used to compare group means. P values less than 0.05 were considered significant.

Results

Effects of Pioglitazone on Cell Mitochondrial Content and Quantity. We used three different approaches to assess whether pioglitazone influences the content or quantity of NT2 cell mitochondria. Our evaluation included real-time PCR determination of relative mtDNA copy number, immunochemical quantification of both mtDNA and nuclear DNA-encoded mitochondrial proteins, and quantitative measurement of citrate synthase activity (a physiologic correlate of cell mitochondrial mass). The real-time PCR data are shown in Fig. 1. We independently analyzed mtDNA copy number for two parts of the mtDNA, the CO1 gene, and the D-loop. In both instances mtDNA copy number was increased. This was the case for pioglitazone exposures of 10, 20, and 40 μM.

The immunochemical quantification studies used a Western blot approach to measure levels of the cytochrome oxidase CO1 subunit and the cytochrome oxidase CO4 subunit. These data are shown in Fig. 2. CO1 is mtDNA-encoded, whereas CO4 is encoded by a nuclear gene, translated in the cytoplasm, and imported into mitochondria. Figure 2 shows levels of both proteins were elevated at subtoxic pioglitazone concentrations. In each case, with 40 μM pioglitazone, there

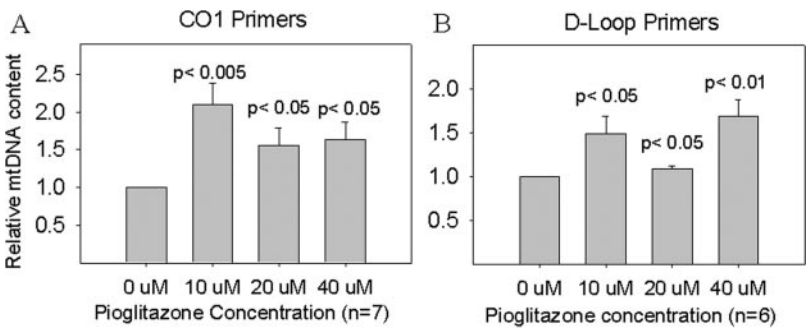

Fig. 1. Long-term pioglitazone treatment increases NT2 cell mtDNA content. Data reflect relative mtDNA content of pioglitazone-treated cells versus that of cells not treated with pioglitazone. The analysis was done using two different mtDNA primer sets. One primer set was to CO1 of the mtDNA (A) and the other was to the D-loop (B).

was increased variance of data and results between concentrations were not significantly different.

Citrate synthase is encoded by a nuclear gene, translated in the cytoplasm, and imported into the mitochondrial matrix. Figure 3 shows the V_{max} of the enzyme was clearly increased at 20 μM pioglitazone. At 40 μM, the citrate synthase V_{max} was actually decreased below baseline.

Effects on Cell Respiration and Electron Transport Chain Function. We used an assay of cell oxygen consumption to assess mitochondrial respiratory rates in pioglitazone-treated cells. Assays were performed using oxygen biosensor plates (Bio-Rad Laboratories), which facilitate quantitative assessments of cell oxygen consumption. Data were analyzed in terms of oxygen consumption rates and absolute oxygen consumption at 1 h (Fig. 4). For cells maintained in medium containing 20 μM pioglitazone, there was an approximate 20 to 30% increase in both cell oxygen consumption rates and absolute oxygen consumption. This was not the case with exposure to 40 μM pioglitazone, suggesting that this concentration induced functional mitochondrial toxicity.

High cell respiration rates could correlate with increased electron transport chain (ETC) enzyme activities. Figure 5 shows this was indeed the case. We determined complex I V_{max} activity in purified mitochondrial fractions prepared from NT2 cells disrupted through nitrogen cavitation, and complex IV (cytochrome oxidase) V_{max} activity in whole NT2 cells. The results of these spectrophotometric biochemical assays are shown in Fig. 5. Complex I activity was increased with 10 μM pioglitazone. With 20 μM pioglitazone, there was a trend toward increased complex I activity that was not statistically significant. At 40 μM, there was a suggested trend toward reduced complex I activity. There was a nonsignificant trend toward increased complex IV activity with 5 μM pioglitazone ($p = 0.075$). Complex IV activity was increased with 10 and 20 μM pioglitazone exposures, but not with exposure to 40 μM pioglitazone.

Effects on Reactive Oxygen Species Production and Oxidative Stress. We used three different approaches to measure peroxide production. First, we used DCF, a peroxide-sensitive fluorescent dye. DCF is localized to cell cytoplasm and provides sensitive measurements of cytoplasmic peroxide levels. Cells that overproduce peroxide can compensate to some extent by up-regulating antioxidant enzyme activities. We felt it was important to determine whether this was indeed happening, and thus we measured GPx activities in our pioglitazone-exposed NT2 cells. Finally, we directly assayed mitochondrial peroxide production using another fluorescent dye, Amplex red.

Figure 6 summarizes the results of these assays. The DCF assay demonstrated a pioglitazone dose-dependent increase in cytoplasmic peroxide production. Associated with this increase in cytoplasmic peroxide production was a concomitant up-regulation of glutathione peroxidase activity, indicating the observed increase in cytoplasmic peroxide levels was enough to induce a cell compensatory response. Paradoxically, we also found a robust reduction in mitochondrial peroxide levels.

Discussion

Long-term exposure to the thiazolidinedione pioglitazone affects mitochondria. The pioglitazone-induced mtDNA increase we observed is consistent with either more mtDNA per mitochondrion or increased mitochondrial number. Likewise, increased ETC protein and citrate synthase activity (per fixed amounts of total cell protein) could reflect denser packaging of cell mitochondrial protein or more mitochondria per cell. We feel in each case that the latter scenario, mitochondrial biogenesis, is more likely. Based also on real time PCR analysis of mtDNA quantity, expression of nuclear-encoded, mitochondria-relevant genes, and expression levels of mtDNA genes other groups previously concluded pioglitazone induces mitochondrial biogenesis in human subcutaneous adipose tissue and cultured preadipocytes (Bogacka et al., 2005; Roses and Saunders, 2006; Roses et al., 2007). If pioglitazone is indeed promoting mitochondrial biogenesis, it

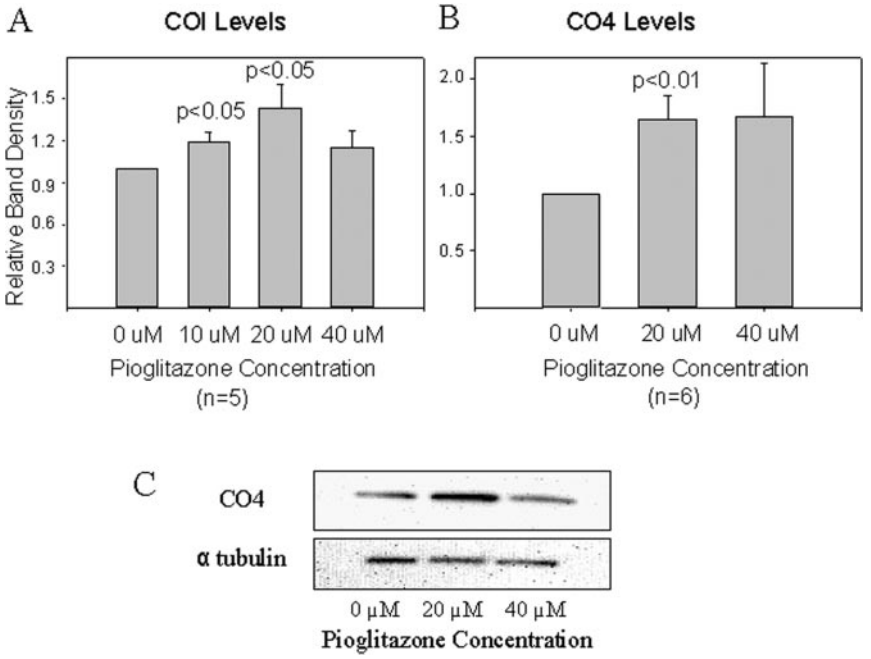

Fig. 2. Levels of electron transport chain subunits are increased by long-term pioglitazone exposure. The graphs compare densitometry readings from Western blots of mitochondrial protein (for CO1) or whole-cell protein (for CO4) prepared from pioglitazone-treated and untreated cells. Mean density values from pioglitazone-treated cells are reported relative to that of untreated cells. A, pioglitazone treatment increased levels of CO1, an mtDNA-encoded electron transport chain subunit. B, pioglitazone treatment increased levels of CO4, a nuclear-encoded electron transport chain subunit. For the CO4 analysis, tubulin was used as an internal loading control, and tubulin levels were equivalent between pioglitazone treated and untreated cells. C, a representative CO4 experiment with its tubulin control.

is worth considering the fact PPARG and NRF-1 transcription factors share a common coactivator, PGC-1α (Scarpulla, 2002). NRF-1 promotes mitochondrial biogenesis. Although our data do not address this possibility, it is worth considering whether thiazolidinedione drugs that mimic the effects of PGC-1α on PPARG also mimic the effects of PGC-1α on NRF-1.

Although NT2 cell citrate synthase activity was increased with long-term exposure to 20 μM pioglitazone, with 40 μM exposure it was decreased from baseline. In vitro pioglitazone studies typically use 10 to 20 μM concentrations. These concentrations exceed clinically achieved serum levels. Budde et al. (2003) determined serum pioglitazone concentrations in pioglitazone-treated diabetics. The mean serum C_{max} was 1.329 μg/ml, or ~3 μM (10 μM = 3.92 μg/ml) (Ito et al., 2003).

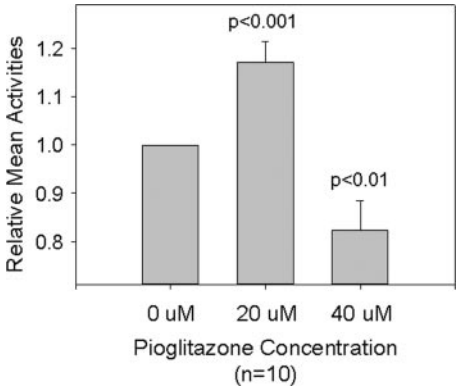

Fig. 3. Citrate synthase activities from pioglitazone-treated and untreated cells. Data were recorded as nanomoles per minute per milligram of protein and in the figure are reported as mean activity of pioglitazone-treated cells relative to that of untreated cells.

We suspect decreased citrate synthase activity at 40 μM pioglitazone reflects toxicity at that concentration. Although our real-time PCR data suggest mitochondrial biogenesis was still promoted at 40 μM pioglitazone, production of functional mitochondria was reduced. Decreased citrate synthase activity may reflect compromised mitochondrial integrity, impaired mitochondrial import, or an oxidative stress-mediated inhibition of the enzyme. Our oxidative stress determinations argue the latter scenario is less likely, because mitochondrial peroxide was reduced at all concentrations of pioglitazone evaluated. Taken together, our studies suggest at sufficient concentrations that pioglitazone induces mitochondrial proliferation via induction of mitochondrial biogenesis, but at clinically toxic concentrations mitochondrial integrity is compromised.

Our oxygen consumption, complex I V_{max}, and complex IV V_{max} data support this view. These parameters were enhanced with long-term 10 to 20 μM pioglitazone exposure but not with 40 μM exposure. If the observed loss of functional enhancement at the higher concentration is indeed a toxicity effect, elucidating the underlying mechanism is worthwhile. Possibilities include the cytoplasmic oxidative stress induced by pioglitazone, altered stoichiometric relationships between nuclear DNA and mtDNA encoded ETC subunits, or drug-induced expression of nuclear genes that influence mitochondrial function.

To better assess dose-response relationships, we tested the effects of 5 μM pioglitazone on complex IV activity. We cannot conclude long-term 5 μM pioglitazone exposure has no effect on mitochondrial biogenesis, but can conclude 5 μM pioglitazone produces at most a less robust response than 10 μM pioglitazone. We therefore assume more pioglitazone is

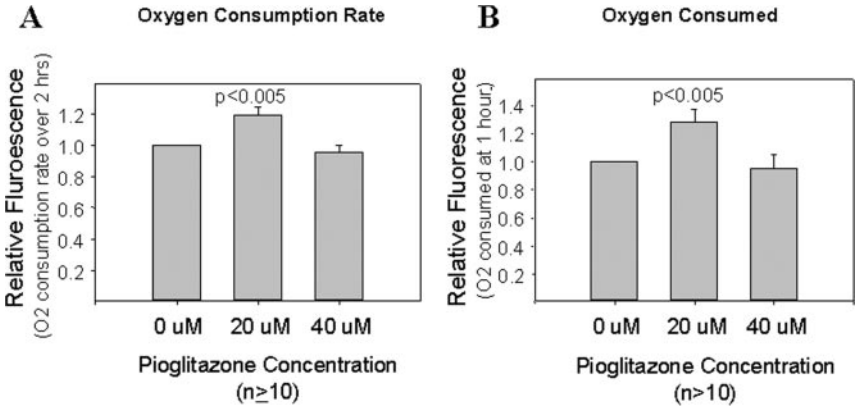

Fig. 4. Relative to untreated cells, oxygen consumption in pioglitazone-treated cells was increased. Data are reported two different ways. A, the oxygen consumption slopes from pioglitazone-treated cells are shown relative to the slope of untreated cells. B, the relative amounts of oxygen consumed over 1 h are shown.

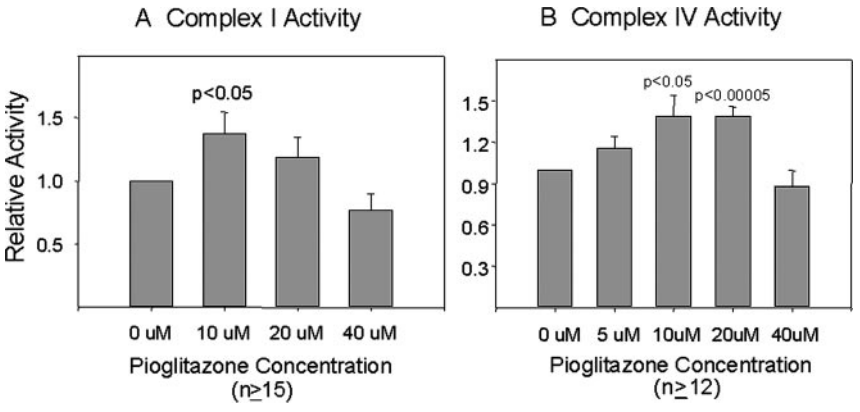

Fig. 5. Relative to untreated cells, electron transport chain V_{max} activities from pioglitazone treated cells are increased. A, complex I activity. B, complex IV activity.

needed to induce mitochondrial biogenesis than is needed to activate PPARG.

Complex IV activity was increased with both 10 and 20 μM pioglitazone. Although the complex I V_{max} was also increased at 10 μM pioglitazone, we did not show this effect with 20 μM pioglitazone. Measuring complex I activity is more technically difficult than measuring complex IV activity, and so this may reflect type II error. On the other hand, this finding may be real. If so, several explanations are possible. Subtle increases in mitochondrial fragility may have begun even with 20 μM pioglitazone, to the point that mitochondrial purification or sonication procedures caused excess disruption of mitochondrial integrity. Complex I consists of 46 bigenomically encoded protein subunits (as opposed to 13 for complex IV) and so may be more sensitive to minor inequities between mitochondrial and nuclear-encoded ETC subunit gene expression (Carroll et al., 2005). Another potential explanation relates to the fact that radical species can negatively regulate ETC function, and complex I is susceptible to this (Riobó et al., 2001). Although cytoplasmic peroxide levels increased in a dose-dependent fashion, mitochondrial peroxide levels did not. We therefore think this latter possibility should not account for the lack of complex I V_{max} increase with 20 μM pioglitazone.

Short-term exposure of isolated mitochondria to thiazolidinediones reduces complex I activity and pyruvate-driven state III respiration (Dello Russo et al., 2003; Brunmair et al., 2004; Scatena et al., 2004; Feinstein et al., 2005). Dello Russo et al. (2003) also found mitochondrial hyperpolarization occurs in cultured rat astrocytes exposed to pioglitazone for 6 h. The data we obtained using a long-term exposure model, in which human NT2 cells were maintained for weeks in pioglitazone, deviate from those of short-term exposure models. Mitochondria in dividing cells over time may respond or adapt to thiazolidinediones differently than mitochondria exposed after removal from cells or after brief intracellular exposures. Our data in no way impugn those from short-term exposure models, as critical methodologic differences distinguish our studies from short-term exposure studies. Different results between these two approaches suggest, though, that mechanisms influencing mitochondrial function in our long-term exposure model ultimately extend beyond those occurring under short-term exposure conditions. A relationship between time-dependent mechanisms may nevertheless exist, because mitochondrial dysfunction is itself associated with mitochondrial biogenesis (Heddi et al., 1999). It is tempting to speculate acute pioglitazone exposure may trigger a secondary, delayed mitochondrial biogenesis.

Observed increases in complex I and IV V_{max} activities could reflect quantitative or qualitative alterations of these enzymes. Our citrate synthase data are relevant in this regard. Dividing complex I and IV activities by citrate synthase activity at least partly corrects ETC V_{max} increases. This suggests increased mitochondrial quantity mostly accounts for ETC activity increases.

Oxidative stress may contribute to thiazolidinedione toxicity (Shishido et al., 2003). In this study, increasing pioglitazone concentrations correlated with cytoplasmic hydrogen peroxide levels. This rise in peroxide occurred despite increased GPx activity. The mechanisms underlying thiazolidinedione-related free radical production are unclear. We considered the possibility increased ETC throughput might secondarily increase oxidative stress. After all, running the ETC of hyperpolarized mitochondria promotes superoxide production. However, in our experiments isolated mitochondria showed reduced peroxide levels, suggesting mitochondria are not responsible for the cytoplasmic increase. Alternative sources of cytoplasmic peroxide include peroxisomes, membrane NADH oxidoreductases, and NADPH oxidase.

Reduced mitochondrial peroxide levels could reflect robust up-regulation of mitochondrial antioxidant enzymes. Alternatively, a disproportionate increase in complex III subunits could reduce ETC "electron leak" and lower superoxide production. Dissociation of electron transport from hydrogen translocation/ADP phosphorylation (uncoupling) requires consideration (Digby et al., 1998; Kelly et al., 1998; Shimokawa et al., 1998; Andrews et al., 2005; Douette and Sluse, 2006).

Insulin resistance in type II diabetes is largely determined by muscle mitochondria (Lowell and Shulman, 2005). Although pioglitazone reduces insulin resistance, the role mitochondria might play in this has not been widely considered. Our experiments used a neuron-like cell line rather than muscle but nevertheless argue that pioglitazone may benefit diabetics by affecting mitochondria. Various neurodegenerative diseases are also associated with ETC enzyme activity

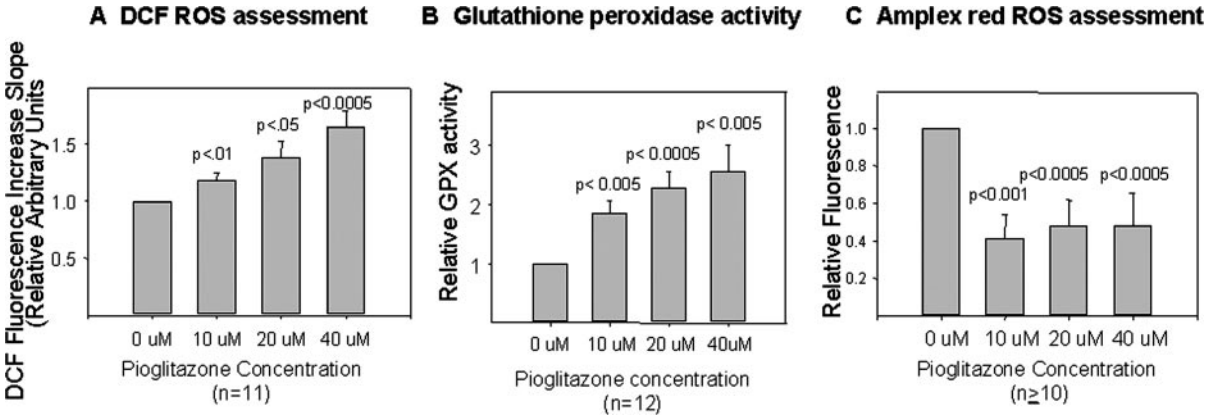

Fig. 6. Cell peroxide production and oxidative stress levels are affected by long-term pioglitazone exposure. A, relative to untreated cells, higher DCF fluorescence in pioglitazone-treated cells indicates higher cytoplasmic peroxide levels. B, relative to untreated cells, pioglitazone-treated cells show increased glutathione peroxidase activity. C, using Amplex red fluorescence as a measure of peroxide, peroxide levels are lower in mitochondria isolated from pioglitazone-treated cells than in mitochondria isolated from untreated cells.

reductions and increased mitochondria-generated oxidative stress (Swerdlow, 2007). The ability of pioglitazone to increase complex I and IV V_{max} activities and reduce mitochondrial peroxide levels in a neuron-like cell line make it interesting from a neurodegenerative disease-therapeutic perspective.

The use of thiazolidinedione drugs for AD was previously advocated (Heneka et al., 2005; Watson et al., 2005; Geldmacher et al., 2006, Landreth, 2006; Risner et al., 2006). Exploratory analyses from a phase II trial of rosiglitazone in AD suggest rosiglitazone might benefit cognition in those not carrying *APOE4* alleles (Risner et al., 2006). It is noteworthy that an apolipoprotein E-mitochondrial nexus exists, because apolipoprotein E C-terminal fragments induce mitochondrial dysfunction (Chang et al., 2005). Interactions between rosiglitazone response and *APOE* in the Risner et al. (2006) trial could support a hypothesis stating that apolipoprotein E fragments may facilitate AD by altering mitochondrial physiology (Roses et al., 2007).

Proposed rationales for trying thiazolidinediones in AD include their effects on insulin, amyloid precursor protein processing, and inflammation. Our data support another rationale, previously proposed by others (Roses et al., 2007), that postulates thiazolidinediones may benefit AD subjects by enhancing mitochondrial function. Our data further suggest thiazolidinediones might benefit other neurodegenerative diseases with mitochondrial dysfunction (Swerdlow, 2007). Current thiazolidinediones, though, do not robustly pass the blood brain barrier. One study reported cerebrospinal fluid concentrations of pioglitazone were only 18% that of serum (Maeshiba et al., 1997; Heneka et al., 2005). Although serum concentrations of pioglitazone and its active metabolites have surpassed 100 μM in animal studies, under clinical conditions serum concentrations are in the 2 to 3 μM range (Budde et al., 2002; Feinstein et al., 2005). Development of thiazolidinedione mimetics capable of crossing the blood-brain barrier seems justified.

Acknowledgments

We thank Takeda Pharmaceuticals (Osaka, Japan) for providing pioglitazone.

References

Andrews ZB, Diano S, and Horvath TL (2005) Mitochondrial uncoupling proteins in the CNS: in support of function and survival. *Nat Rev Neurosci* **6:**829–840.
Bogacka I, Xie H, Bray GA, amd Smith SR (2005) Pioglitazone induces mitochondrial biogenesis in human subcutaneous adipose tissue in vivo. *Diabetes* **54:**1392–1399.
Brunmair B, Staniek K, Gras F, Scharf N, Althaym A, Clara R, Roden R, Gnaiger E, Nohl H, Waldhausl W, et al. (2004) Thiazolidinedines, like metformin, inhibit respiratory complex I. A common mechanism contributing to their antidiabetic actions? *Diabetes* **53:**1052–1059.
Budde K, Neumayer HH, Fritsche L, Sulowicz W, Stompor T, and Eckland D (2003) The pharmacokinetics of pioglitazone in patients with impaired renal function. *J Clin Pharmacol* **55:**368–374.
Carroll J, Fearnley IM, Skehel JM, Runswick MJ, Shannon RJ, Hirst J, and Walker JE (2005) The post-translational modifications of the nuclear encoded subunits of complex I from bovine heart mitochondria. *Mol Cell Proteomics* **4:**693–699.
Chang S, ran Ma T, Miranda RD, Balestra ME, Mahley RW, Huang Y (2005) Lipid- and receptor-binding regions of apolipoprotein E4 fragments act in concert to cause mitochondrial dysfunction and neurotoxicity. *Proc Natl Acad Sci USA* **102:** 18694–18699.
Dello Russo C, Gavrilyuk V, Weinberg G, Almeida A, Bolanos JP, Palmer J, Pelligrino D, Galea E, and Feinstein DL (2003) Peroxisome proliferator-activated receptor γ thiazolidinedione agonists increase glucose metabolism in astrocytes. *J Biol Chem* **278:**5823–5836.
Digby JE, Montague CT, Sewter CP, Sanders L, Wilkison WO, O'Rahilly S, and Prins JB (1998) Thiazolidinedione exposure increases the expression of uncoupling protein 1 in cultured human preadipocytes. *Diabetes* **47:**138–141.
Douette P and Sluse FE (2006) Mitochondrial uncoupling proteins: new insights from functional and proteomic studies. *Free Radic Biol Med* **40:**1097–1107.
Feinstein DL, Spagnolo A, Akar C, Weinberg G, Murphy P, Gavrilyuk V, and Dello Russo C (2005) Receptor-independent actions of PPAR thiazolidinedione agonists: is mitochondrial function the key? *Biochem Pharmacol* **70:**177–188.
Fiskum G, Rosenthal RE, Vereczki V, Martin E, Hoffman GE, Chinopoulos C, and Kowaltowski A (2004) Protection against ischemic brain injury by inhibition of mitochondrial oxidative stress. *J Bioenerg Biomembr* **36:**347–352.
Geldmacher DS, Fritsch T, McClendon MJ, Lerner AJ, and Landreth GE (2006) A double-blind, placebo controlled, 18 month pilot study of the PPAR-gamma agonist pioglitazone in Alzheimer's disease. *Alzheimers Dement* **2(Suppl)**:S366.
Heddi A, Stepien G, Benke PJ, and Wallace DC (1999) Coordinate induction of energy gene expression in tissues of mitochondrial disease patients. *J Biol Chem* **274:**22968–22976.
Heneka MT, Sastre M, Dumitrescu-Ozimek L, Hanke A, Dewachter I, Kuiperi C, O'Banion K, Klockgether T, Van Leuven F, and Landreth GE (2005) Acute treatment with the PPARgamma agonist pioglitazone and ibuprofen reduces glial inflammation and Abeta1–42 levels in APPV717I transgenic mice. *Brain* **128:** 1442–1453.
Ito H, Makano A, Kinoshita M, and Matsumori A (2003) Pioglitazone, a peroxisome proliferator-activated receptor-(agonist, attenuates myocardial ischemia/reperfusion injury in a rat model. *Lab Investig* **83:**1715–1721.
Kelly LJ, Vicario PP, Thompson GM, Caldelore MR, Doebber TW, Ventre J, Wu MS, Meurer R, Forrest MJ, Conner MW, et al. (1998) Peroxisome proliferator-activated receptors gamma and alpha mediate in vivo regulation of uncoupling protein (UCP-1, UCP-2, UCP-3) gene expression. *Endocrinology* **139:**4920–4927.
Landreth G (2006) PPARγ agonists as new therapeutic agents for the treatment of Alzheimer's disease. *Exp Neurol* **199:**245–248.
Lowell BB and Shulman GI (2005) Mitochondrial dysfunction in type II diabetes. *Science (Wash DC)* **307:**384–387.
Maeshiba Y, Kiyota Y, Yamashita K, Yoshimura Y, Motohashi M, and Tanayama S (1997) Disposition of the new antidiabetic agent pioglitazone in rats, dogs, and monkeys. *Arzneimittel-Forschung* **47:**29–35.
May-Panloup P, Vignon X, Chretien MF, Heyman Y, Tamassia M, Malthiery Y, and Reynier P (2005) Increase of mitochondrial DNA content and transcripts in early bovine embryogenesis associated with ation of mtTFA and NRF1 transcription factors. *Reprod Biol Endocrinol* **3:**65.
Parker WD Jr, Filley CM, and Parks JK (1990) Cytochrome oxidase deficiency in Alzheimer's disease. *Neurology* **40:**1302–1303.
Riobó NA, Clementi E, Melani M, Boveris A, Cadenas E, Moncada S, and Poderoso JJ (2001) Nitric oxide inhibits mitochondrial NADH:ubiquinone reductase activity through peroxynitrite formation. *Biochem J* **359:**139–145.
Risner ME, Saunders AM, Altman JF, Ormandy GC, Craft S, Foley IM, Zvartau-Hind ME, Hosford DA, and Roses AD (2006) Efficacy of rosiglitazone in a genetically defined population with mild-to-moderate Alzheimer's disease. *Pharmacogenomics J* **6:**246–254.
Roses AD and Saunders AM (2006) Perspective on a pathogenesis and treatment of Alzheimer's disease. *Alzheimers Dement* **2:**59–70.
Roses AD, Saunders AM, Huang Y, Strum J, Weisgraber KH, and Mahley RW (2007) Complex disease-associated pharmacogenetics: drug efficacy, drug safety, and confirmation of a pathogenetic hypothesis (Alzheimer's disease). *Pharmacogenomics J* **7:**10–28.
Scarpulla RC (2002) Transcriptional activators and coactivators in the nuclear control of mitochondrial function in mammalian cells. *Gene* **286:**81–89.
Scatena R, Bottoni P, Martorana GE, Ferrari F, De Sole P, Rossi C, and Giardina B (2004) Mitochondrial respiratory chain dysfunction, a non-receptor-mediated effect of synthetic PPAR-ligands: biochemical and pharmacological implications. *Biochem Biophys Res Commun* **319:**967–973.
Shimokawa T, Kato M, Watanabe Y, Hirayama R, Kurosaki E, Shikama H, and Hashimoto S (1998) In vivo effects of pioglitazone on uncoupling protein-2 and −3 mRNA levels in skeletal muscle of hyperglycemic KK mice. *Biochem Biophys Res Commun* **251:**374–378.
Shishido S, Koga H, Harada M, Kumemura H, Hanada S, Taniguchi E, Kumashiro R, Ohira H, Sato Y, Namba M, et al. (2003) Hydrogen peroxide overproduction in megamitochondria of troglitazone-treated human hepatocytes. *Hepatology* **37:** 136–147.
Swerdlow RH and Kish SJ (2002) Mitochondria in Alzheimer's disease. *Int Rev Neurobiol* **53:**341–385.
Swerdlow RH (2007) Mitochondria in cybrids containing mtDNA from persons with mitochondriopathies. *J Neurosci Res*, in press.
von Wurmb-Schwark N, Higuchi R, Fenech AP, Elfstroem C, Meissner C, Oehmichen M, and Cortopassi GA (2002) Quantification of human mitochondrial DNA in a real time PCR. *Forensic Sci Int* **126:**34–39.
Watson GS, Cholerton BA, Reger MA, Baker LD, Phymate SR, Asthana S, Fishel MA, Kulstad JJ, Green PS, Cook DG, et al. (2005) Preserved cognition in patients with early Alzheimer disease and amnestic mild cognitive impairment during treatment with rosiglitazone: a preliminary study. *Am J Geriatr Psychiatry* **13:** 950–958.
Wu Z, Puigserver P, Andersson U, Zhang C, Adelmant G, Mootha V, Troy A, Cinti S, Lowell B, Scarpulla RC, et al. (1999) Mechanisms controlling mitochondrial biogenesis and respiration through the thermogenic coactivator PGC-1. *Cell* **98:**115–124.
Yki-Järvinen H (2004) Thiazolidinediones. *N Engl J Med* **351:**1106–1118, .

Address correspondence to: Dr. Russell H. Swerdlow, #800394, Department of Neurology, McKim Hall, 1 Hospital Drive, Charlottesville, VA 22908. E-mail: rhs7e@virginia.edu